OncoTargets and Therapy

Dovepress
open access to scientific and medical research

Open Access Full Text Article

ORIGINAL RESEARCH

RETRACTED ARTICLE: Downregulation of ribophorin II suppresses tumor growth, migration, and invasion of nasopharyngeal carcinoma

This article was published in the following Dove Press journal:
OncoTargets and Therapy

Feilong Hong
Yong Li
Haifeng Ni
Jing Li

Department of Otolaryngology, Hangzhou First People's Hospital, Hangzhou, China

Background: It has been reported that ribophorin II (RPN2) expression is increased in many cancers, but the role of RPN2 in nasopharyngeal carcinoma (NPC) remains unclear.

Patients and methods: This study found that the expression of RPN2 is increased dramatically in NPC tissues of patients compared with that in the adjacent normal tissues. This study attempted at understanding the effect of siRNA-RPN2 treatment on the migration and invasion of NPC cell lines CNE2 and HNE1.

Results: RT-PCR and Western blotting showed that RPN2 was highly expressed in CNE2 and HNE1 cells. siRNA-RPN2 treatment significantly inhibited cell viability at 24 and 48 h compared with the control group. Results of the transwell assay showed that, compared to the control groups, migration and invasion of the cells treated with siRNA-RPN2 decreased markedly. In addition, compared to the control groups, caspase-3, caspase-9, and E-cadherin expression levels increased and MMP2 expression decreased significantly in the siRNA-RPN2-treated group. Phosphorylation of AKT and PI3K was also inhibited after siRNA-RPN2 treatment.

Conclusion: siRNA-RPN2 can effectively inhibit the invasion and migration of human NPC cells via AKT/PI3K signaling. This can serve as a novel strategy for NPC treatment.

Keywords: siRNA-RPN2, nasopharyngeal carcinoma, migration, invasion, MMP2, MMP9

Introduction

Nasopharyngeal carcinoma (NPC), an epithelial malignancy of the head and neck, is one of the most common malignant tumors in Southeast Asia and southern China, where the incidence rate is approximately 25 cases per 100,000 individuals.[1–3] Approximately 80,000 new cases and 50,000 deaths are reported annually all over the world.[4,5] Although the overall survival has improved by using intensity-modulated radiation therapy or chemotherapy, prognosis for patients with NPC remains very poor, due to disease recurrence and distant metastasis.[6] The development of distant metastasis remains intractable, and ultimately results in death.[7] Therefore, it is imperative to fully elucidate the molecular mechanism(s) involved in the migration and invasion of NPC cells to facilitate the development of novel therapeutic strategies.

Ribophorin II (RPN2) is a part of an N-oligosaccharyl transferase complex.[8,9] RPN2 can mediate CD63 glycosylation, which regulates MDR1 localization and cancer malignancy, as well as drug resistance and invasion in breast cancer.[9] RPN2 immunostaining exhibited a significant association with stage III/IV tumors, distant metastasis, and poor differentiation in colorectal cancer.[10] RPN2 expression confers early and distant recurrence, and results in poor survival in non-small cell lung cancer

Correspondence: Yong Li
Department of Otolaryngology, Hangzhou First People's Hospital, No 261 Huansha Road, Hangzhou 310000, China
Tel +86 571 5600 8888
Email hongfeilong_1014@163.com

submit your manuscript | www.dovepress.com
Dovepress
http://dx.doi.org/10.2147/OTT.S158355

patients, while RPN2 silencing suppresses cell proliferation and invasiveness.[8] The correlation between RPN2 and NPC has not been reported.

In this study, we first observed that the expression of RPN2 was significantly higher in the NPC tissue than in the peritumor tissue. Thus, it would be interesting to determine whether RPN2 plays a role in the development and metastasis of NPC. In the present study, we attempted to explore the effect(s) of siRNA-RPN2 silencing on the migration and invasion of NPC cells which expressed RPN2. Moreover, the underlying mechanisms involved were also investigated to provide novel insights into potential NPC therapeutic strategies.

Patients and methods

Patients and tissue samples

Written informed consent was obtained from all participants before the study. Sixty-eight patients with NPC admitted to the Hangzhou First People's Hospital were enrolled for this study, and our study was approved by the independent ethics committee of the Hangzhou First People's Hospital. Preoperative clinical and pathological follow-up data were provided by all patients. All samples from patients were collected according to the procedures approved by the institutional review board of the independent ethics committee of the Hangzhou First People's Hospital. Normal nasopharyngeal tissues present adjacent to the cancerous tissues were also collected, which acted as negative controls.

Immunohistochemistry

After being dewaxed in xylene and rehydrated through graded alcohol to distilled water, NPC specimen sections were immersed in 3% hydrogen peroxide for 15 min at room temperature to prevent endogenous peroxidase activity. Next, the sections were boiled in the antigen retrieval solution (citrate, pH=6) for 4 min in a pressure cooker for antigen retrieval. After being cooled down to 26°C, the sections were incubated with diluted rabbit anti-RPN2 antibody (1:200; Proteintech Group, Wuhan, China) overnight at 4°C. The next day, after rinsing thrice with phosphate buffered saline with Tween 20 (PBST), the sections were incubated with the secondary antibody for 30 min at 37°C. Next, the sections were rinsed with PBST three times, and 3,3-diaminobenzidine staining was performed for 2 min for targeted protein identification. The sections were counterstained with hematoxylin to stain the nucleus. After rinsing for 2 h under flowing water and dehydrating at 37°C, the specimen sections were mounted using Neutral Balsam for preservation.

Cell culture

Human NPC cells, namely CNE2, CNE2, HNE1, SUNE-1, and 5-8F cells, were obtained from the Shanghai Cell Bank (Chinese Academy of Sciences, Shanghai, China) and cultured in RPMI 1640 medium (Gibco, Thermo Fisher Scientific, Waltham, MA, USA) containing 10% fetal bovine serum and 1% penicillin/streptomycin (Invitrogen, Thermo Fisher Scientific) at 37°C in 5% CO_2.

siRNA transfection

siRNA-RPN2 was designed and synthesized by Genepharma (Shanghai, China). The interference sequence is 5′-GCA GAGCAGAGCAGTAGATTGG A-3′. The NPC cells, CNE2 and HNE1, were selected for transfection. After transfection, RPN2 expression was confirmed using reverse transcription polymerase chain reaction (RT-PCR) and Western blotting. For siRNA transfection, the cells were seeded onto 12-well tissue culture plates at a density of 6×10^4 cells/well. When the cells were 70% confluent, they were transfected with the RPN2 siRNA (siRPN2) or control siRNA (siNC), according to the manufacturer's instructions. After 48 h, the transfected cells were collected and processed for the subsequent experiments.

Cell viability assay

The effect of siRNA-RPN2 treatment on CNE2 and HNE1 cell viability was evaluated using the cell counting kit-8 (CCK-8) assay. Briefly, 0, 12-, 24-, 48-, and 72-h post-transfection, the cells were seeded at a density of 4×10^3 cells/well in 96-cell plates and incubated for the indicated time periods. Next, 20 µL CCK-8 was added to each well and the cells were incubated for 1 h. The OD values were recorded using a microplate reader (Thermo Fisher Scientific) at 450 nm.

Cell cycle assay

After transfection for 48 h, the cells were harvested, washed with PBS, and fixed with 70% ethanol at 4°C overnight. Next, the cells were washed with PBS and resuspended in the RNase A–propidium iodide solution (100 mg/mL RNase A and 5 µg/mL propidium iodide). The cells were incubated at room temperature for 1 h. Stained cells were analyzed using the FACScan flow cytometer (BD Biosciences, Mountain View, CA, USA).

Cell apoptosis assay

Cell apoptosis was detected using the annexin V/PI fluorescence-activated cell sorting (FACS) assay, as described

previously. Briefly, the cells (3×10^5 cells/well) were harvested and washed in cold PBS. After fixing with 70% ethanol, the cells were treated with RNase (5 mmol/L) and incubated for 10–15 min in the dark at 37°C. Subsequently, they were stained with 195 µL Annexin V and 5 µL PI. The fluorescence intensities were determined using fluorescence-activated cell sorting (FACS) to analyze the percentage of apoptotic cells.

Cell migration and invasion assays

The cell migration assay was performed using a 24-well transwell chamber with a pore size of 8 µm (Sigma-Aldrich, Munich, Germany). Then, 5×10^4 siRNA-RPN2-transfected cells, mock cells, and non-transfected cells were resuspended in a serum-free medium and transferred to the upper chamber. The lower chamber was filled with a medium containing 10% fetal bovine serum. After 24-h cultivation, the number of cells stained by 0.1% crystal violet was counted visually under a microscope (OLYMPUS, Hamburg, Germany). The cell invasion assay was performed using the same procedure, except that the upper chamber was coated with matrigel. Results from three independent experiments were averaged and reported.

Quantitative reverse transcription (qRT)-PCR

Total RNA was extracted from transfected cells, mock cells, and non-transfected cells and reverse transcribed to cDNA using the First Strand cDNA Synthesis kit (Sigma-Aldrich) according to the manufacturer's protocol. The PCR cycling conditions were as follows: 95°C for 10 min, followed by 40 cycles of denaturation at 95°C for 15 s and annealing/extension at 60°C for 45 s. The ABI 7300 thermocycler (Applied Biosystems, Foster City, CA, USA) and SYBR Premix Ex Taq kit (Takara, Beijing, China) were used.

Western blot analysis

The concentration of protein extracted from cell samples was determined using the BCA assay (Beyotime). Next, the proteins were subjected to SDS-polyacrylamide gel electrophoresis and electroblotted onto polyvinylidene fluoride membranes. Following blocking with 5% non-fat dry milk in PBS for 1 h, the blotting membranes were probed overnight at 4°C with the following antibodies individually: anti-caspase-3, anti-caspase-9, anti-E-cadherin, anti-MMP2, anti-MMP9, anti-PI3K, anti-AKT, anti-p-PI3K, and anti-p-AKT antibodies. The polyvinylidene fluoride membrane was exposed to an X-ray film, and immunoreactive bands were detected by reaction with the ECL detection system reagents (Amersham, Arlington Heights, IL, USA).

Xenograft model experiments

All experimental protocols involving animals were approved by the institutional animal care and use committee of the Hangzhou First People's Hospital and performed following the Guide for the Care and Use of Laboratory Animals issued by Institute of Laboratory Animal Resources. Four-week-old male severe combined immunodeficiency (SCID) mice were purchased from Beijing HFK Bioscience Co. Ltd. (Beijing, China). Cells transfected with siRNA-RPN2 (Genecopeia, Rockville, MD, USA) were injected into the mice subcutaneously (1×10^6 cells per mouse). Tumor growth in the mice was monitored every 5 days. All mice were euthanized after 40 days, following which, the tumor nodules in the mice were removed. Tumor sizes were measured using a caliper, and tumor volume was calculated using the following equation: tumor volume (mm^3) = length (mm) × width (mm)^2/2.

Statistical analysis

All results represent the mean±SD of three independent experiments. Statistical analysis was performed using the SPSS 13.0 statistical package, and data were subjected to one-way analysis of variance (ANOVA), followed by Dunnett's test. A P-value<0.05 was considered to be statistically significant.

Results

High expression of RPN2 in tumor tissue

To verify the biological role of RPN2 in NPC, the expression levels of RPN2 in tissues of NPC patients were evaluated using RT-PCR and IHC. As shown in Figure 1A, the mRNA expression of RPN2 was higher in the NPC tissues than in the adjacent normal tissues ($P<0.01$). IHC analysis also showed that the expression of RPN2 was higher in the NPC tissues than in the adjacent normal tissues (Figure 1B). These results indicated that RPN2 overexpression may result in the initiation and/or progression of NPC.

siRPN2 inhibits cell proliferation of NPC cell lines

RPN2 mRNA was silenced in CNE2 and HNE1 cell lines, as described previously. The interference efficient was then identified using RT-PCR and Western blotting. Transfection with siRNA-RPN2 resulted in a marked decrease in RPN2 mRNA and protein levels in the siRNA-RPN2 group, compared to the control group and mock group, which confirmed that siRNA-RPN2 was effective in silencing RPN2 expression (Figure 1C and D).

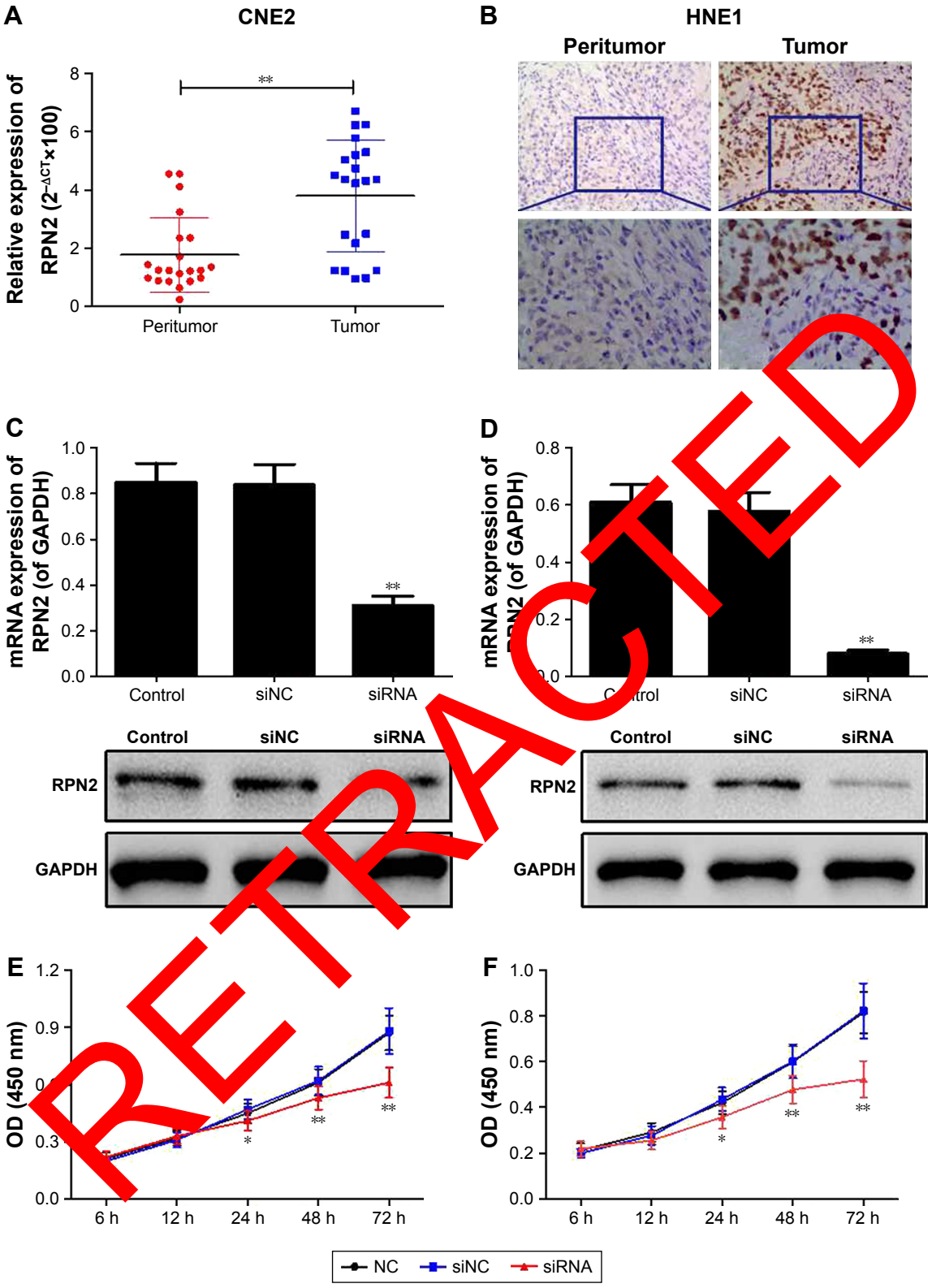

Figure 1 RPN2 expression in NPC tissues and siRNA-RPN2 inhibited cell proliferation of NPC cells. (**A**) mRNA expression of RPN2 in 68 NPC tissues and adjacent normal tissue was determined by RT-PCR. (**B**) Protein expression of RPN2 in NPC tissues and adjacent normal tissue was identified by IHC analysis. Expression of RPN2 was down-regulated in both CNE2 (**C**) and HNE1 (**D**) cells. Cell proliferation in CNE2 (**E**) and HNE1 (**F**) cells was detected by CCK-8 assay.

Notes: Data were presented as mean±SD, *$P<0.05$, **$P<0.01$ compared with the control group.

Abbreviations: RPN2, ribophorin II; NPC, nasopharyngeal carcinoma; RT-PCR, reverse transcription polymerase chain reaction; IHC, immunohistochemistry; CCK-8, cell counting kit-8; SD, standard deviation; OD, optical density.

The effect of siRNA-RPN2 treatment on cell viability measured using the CCK-8 assay is shown in Figure 1E and F. Compared to the control and mock cell groups, cell viability significantly ($P<0.05$) decreased in the siRNA-RPN2 group 24-, 48-, and 72-h post-transfection.

Decrease in RPN2 expression induces cell cycle arrest and apoptosis

To explore the potential mechanism(s) by which RPN2 suppresses NPC cell growth, we evaluated the cell cycle distribution of siRNA-RPN2 transfected cells and siRNA-NC cells using flow cytometry. It was observed that knockdown of RPN2 in the CNE2 and HNE1 cells resulted in an increase in the number of cells in the G0–G1 phase (CNE2, 61.1%±1.1%; HNE1, 59.4%±2.34%) and a decrease in those in the S phase (CNE2, 28.9%±2.32%; HNE1, 29.65%±1.32%), as compared to the siRNA-NC-transfected cells (CNE2: G0–G1, 33.25%±2.09%; S, 55.14%±1.72%; HNE1: G0–G1, 31.18%±1.57%; S, 57.22%±1.67%) (Figure 2A). Additionally, results from the annexin V/PI assay showed that, compared to siRNA-NC-transfected cells (CNE2, 9.77%±1.24%; HNE1, 8.74%±1.14%), the CNE2 and HNE1 cells transfected with

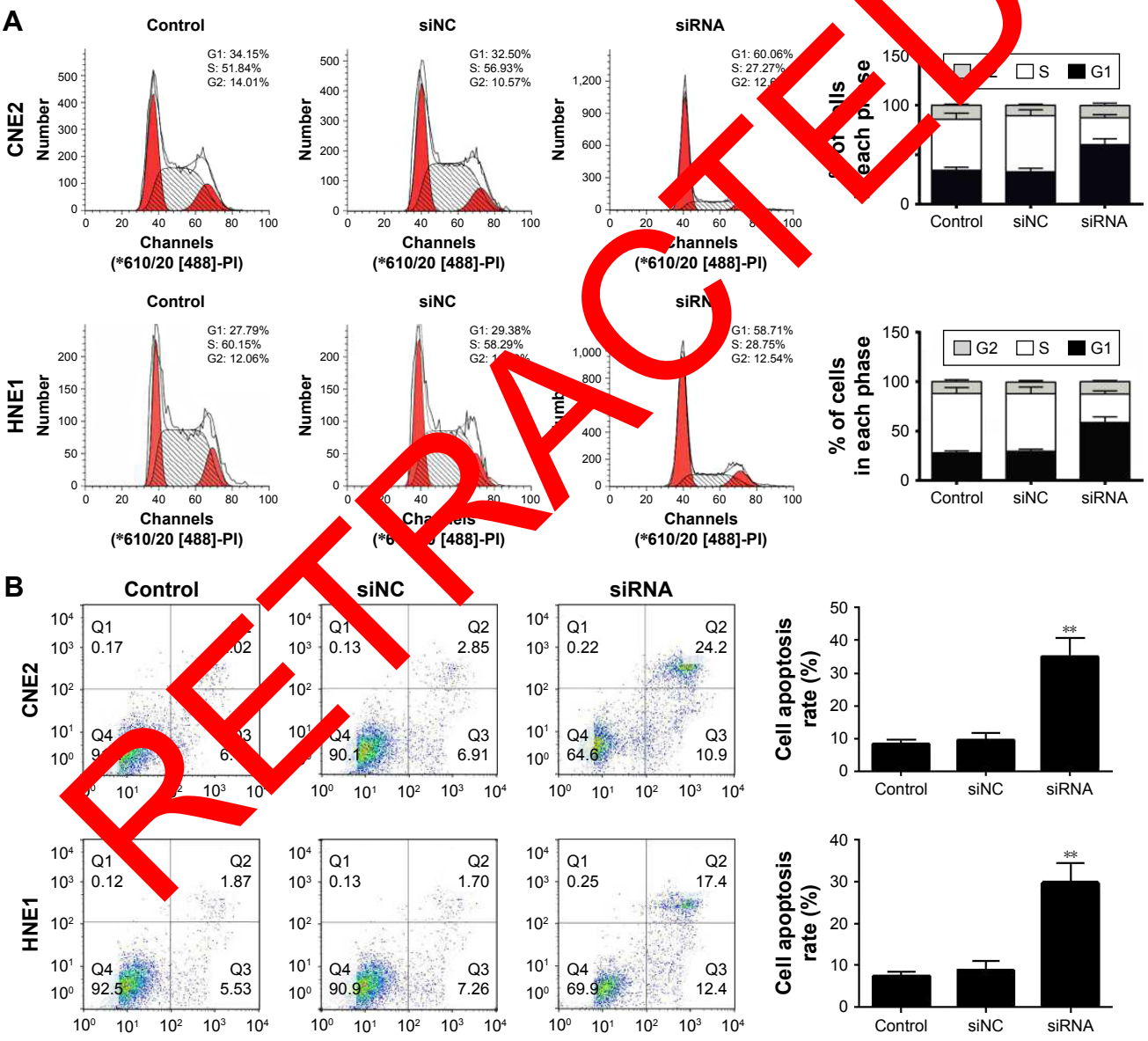

Figure 2 Downregulation of RPN2-induced cell cycle G1 arrest and cell apoptosis. After siRNA-RPN2 transfection for 48 h, cell cycle (**A**) and cell apoptosis (**B**) of CNE2 and HNE1 were identified by flow cytometry.

Note: Data were presented as mean±SD, $^{**}P<0.01$ compared with the control group.

Abbreviation: RPN2, ribophorin II.

siRNA-RPN2 (CNE2, 33.5%±2.76%; HNE1, 28.7%±1.89%) showed increased apoptosis (Figure 2B). Taken together, these data suggested that RPN2 promotes cell proliferation and suppresses apoptosis in NPC cells in vitro.

siRNA-RPN2 inhibits tumor growth in vivo

We investigated the effects of siRNA-RPN2 treatment on repressing tumor growth in vivo. NPC cells transfected with siRNA-RPN2 or a negative control were subcutaneously injected into SCID mice. After 40 days, the mice were euthanized, and RPN2 expression levels in their tissues were measured. The expression of RPN2 was observed to be lower in the group treated with siRNA-RPN2 than in the siNC group. Tumors with lower RPN2 expression showed slower growth and were smaller in size than control tumors (Figure 3). The average tumor weight was approximately 2.3-fold lower in the miR-148a-overexpressing tumors than in the negative controls. These results suggested that siRNA-RPN2 treatment may inhibit NPC cell growth in vivo.

Effects of siRNA-RPN2 treatment on NPC cell migration and invasion

Cell invasion and migration are crucial factors for cancer metastasis.[10] The transwell assay was employed to investigate the effect of siRNA-RPN2 treatment on the migration and invasion of CNE2 and HNE1 cells. As shown in Figure 4A and B, transfection with siRNA-RPN2 resulted in significant lowering of the migration ability of CNE2 and HNE1 cells. Similarly, the transwell invasion assay demonstrated that the invasion abilities of CNE2 and HNE1 cells transfected with siRNA-RPN2 were notably lower than those of the control and mock cells (Figure 4C and D). These results indicated that siRNA-RPN2 treatment significantly inhibited the migration and invasion of CNE2 and HNE1 cells.

siRNA-RPN2 regulates the expression of caspase-3, caspase-9, E-cadherin, and MMP2

Caspase-3, caspase-9, E-cadherin, and MMP2 expressions were monitored by Western blot analysis. Results showed that, compared to the siNC group, the siRNA-RPN2 treated group showed a significant increase in the expression of caspase-3, caspase-9, and E-cadherin in both the CNE2 and HNE1 cells ($P<0.05$, Figure 5A and B). MMP2 expression decreased significantly in NPC cells following siRNA-RPN2 treatment ($P<0.05$, Figure 5C and D). Therefore, inhibition of cell invasion and migration mediated by E-cadherin and MMP2 may play an important role in inhibiting NPC metastasis.

SiRNA-RPN2 suppressed the phosphorylation of PI3K/AKT signaling

The phosphorylation of PI3K/AKT signaling plays a crucial role in NPC occurrence and pathogenesis. Therefore, we

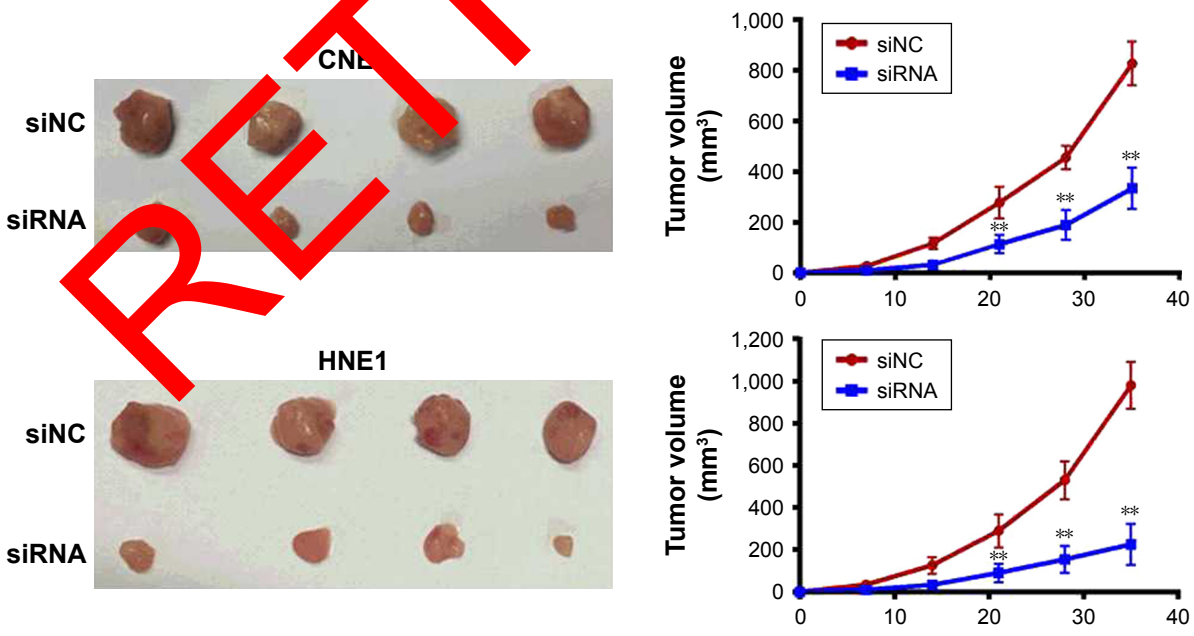

Figure 3 siRNA-RPN2 inhibits tumor growth in vivo. CNE2 and HNE1 cells transfected with siRNA-RPN2 were injected subcutaneously into SCID mice. Representative photograph of xenograft tumors and growth curve for tumor volumes were presented.
Note: Data were presented as mean±SD, $^{**}P<0.01$ compared with the control group.
Abbreviations: RPN2, ribophorin II; SCID, severe combined immunodeficiency.

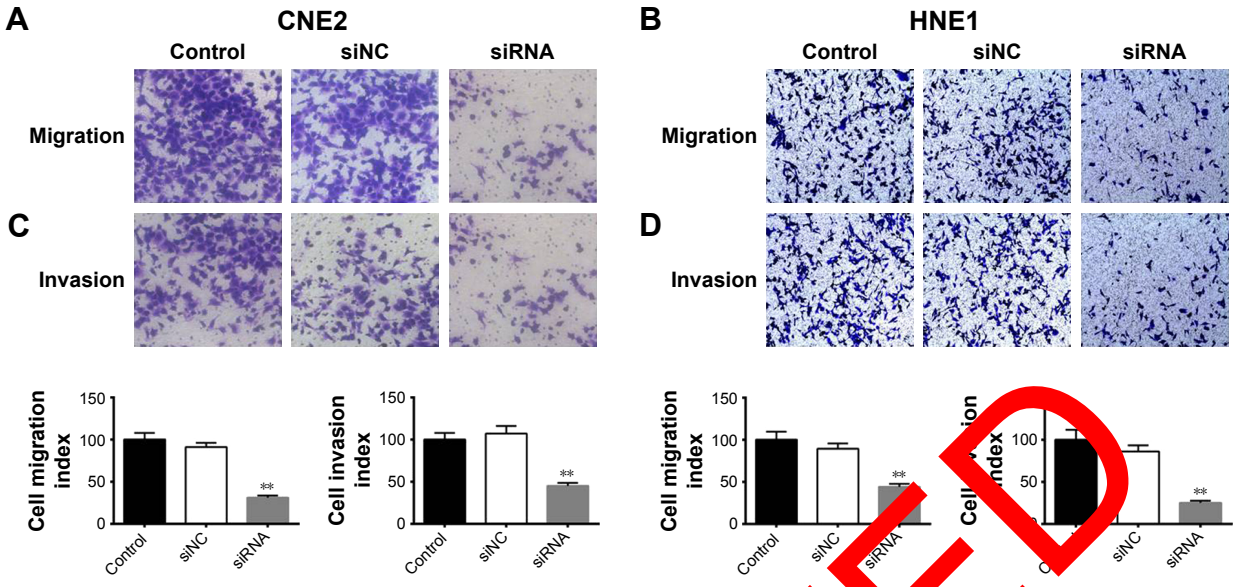

Figure 4 Effect of siRNA-RPN2 on invasion and migration of NPC cells. (**A** and **B**) The migration ability of CNE2 cells following transfection of siRNA-RPN2 for 48 h was identified by transwell assay. (**C** and **D**) After siRNA-RPN2 transfection for 48 h, cell invasion was identified as previously described.
Notes: Data are expressed as the mean±SD, n=6, $^{**}P<0.01$ compared with the control cells.
Abbreviations: RPN2, ribophorin II; NPC, nasopharyngeal carcinoma.

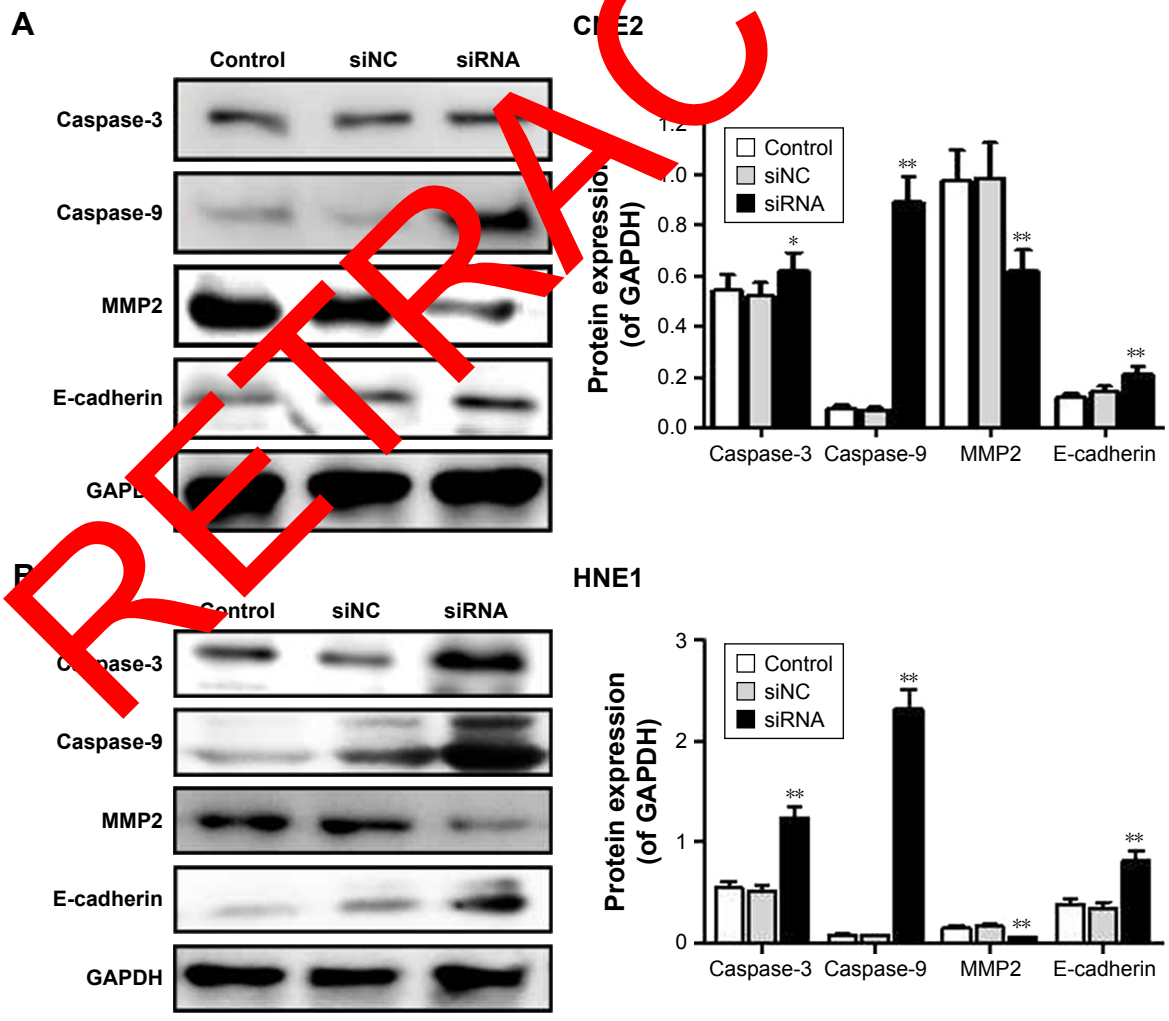

Figure 5 (*Continued*)

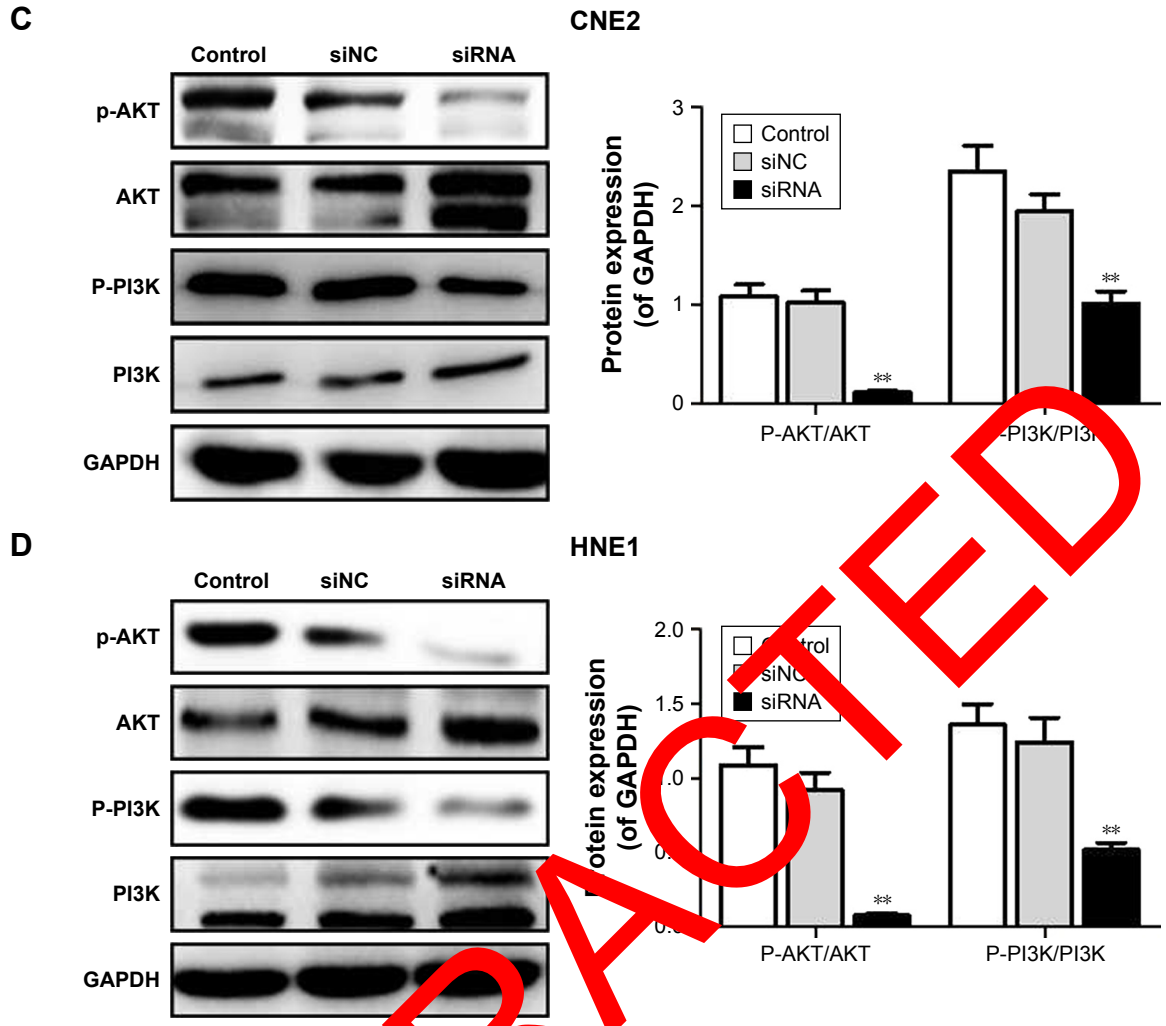

Figure 5 Effect of siRNA-RPN2 on expressions of caspase-3, caspase-9, E-cadherin, and MMP2 and the phosphorylation of PI3K/AKT. (**A** and **B**) After 48 h of siRNA-RPN2 treatment, the protein levels of caspase-3, caspase-9, E-cadherin, and MMP2 in CNE2 and HNE1 cells were analyzed by Western blot. (**C** and **D**) The phosphorylation of PI3K/AKT in CNE2 and HNE1 cells was analyzed by Western blot. GAPDH also detected as the control of sample loading.
Note: Data were presented as mean±SD, *P<0.05, **P<0.01 compared with the control group.
Abbreviations: RPN2, ribophorin II; OD, optical density; SD, standard deviation.

analyzed the effect of siRNA-RPN2 treatment on phosphorylation of PI3K and AKT. We demonstrated that, compared to the siNC and control group, the siRNA-RPN2-treated group showed significantly higher inhibition of AKT and PI3K phosphorylation in the CNE2 and HNE1 cells (P<0.05, Figure 5B).

Discussion

Abnormal expression of RPN2 has been reported in breast cancer, non-small cell lung cancer, gastric cancer, colorectal cancer, and prostatic carcinoma.[11–13] In the present study, we observed a marked increase in RPN2 expression in NPC tissues. The subsequent experiments were designed to explore the effect of siRNA-RPN2 treatment on tumor migration and invasion in NPC. CNE2 and HNE1 were selected for further investigation and validating the high expression of RPN2. siRNA-RPN2 treatment effectively inhibited cell proliferation (in vivo and in vitro), and suppressed the invasion and migration of CNE2 and HNE1 cells. siRNA-RPN2 treatment also effectively induced cell apoptosis, and cell cycle arrest in the G1 phase. The critical role of siRNA-RPN2 in NPC cell growth, invasion, and migration encouraged us to explore the potential mechanism(s) responsible for the aforementioned observations by measuring the changes in expression of relevant genes and proteins. Zhang et al[10] reported that RPN2 regulated colorectal cell proliferation through mediating the glycosylation of EGFR. Fujita et al[8] demonstrated that RPN2 promoted cell proliferation and inhibited cell apoptosis by regulation of Bax/Bcl-2 in non-small cell lung cancer. In this study, we identified the

expression of caspase-3/-9. Caspase-3 and caspase-9 are known to participate in mitochondrial apoptosis, which mediates the apoptotic cascade reaction.[14–16] Caspase-3 is a downstream target in the mitochondrial apoptosis pathway. Activated caspase-8 can lead to the release of caspase-9 and then give rise to the activation of caspase-3, and ultimately to induce apoptosis.[16] Therefore, we detected the caspase-3/-9 expressions after cells transfected with RPN2 siRNA. E-cadherin expression is known to decrease in several carcinoma cells. Further, the extracellular matrix also gets destroyed, which results in tumor migration and invasion.[17,18] Tumor cell invasion and metastasis are characteristic features of malignant phenotypes and require regulated expression of MMPs. Among all MMPs, MMP2 has been suggested to have well-characterized roles in cancer cell invasion and metastasis.[19,20] We also provided evidence suggesting that the mechanism underlying the aforementioned effects was related to the inhibition of expression of MMP2, which is known to play a major role in tumor invasion and metastasis by proteolyzing the extracellular matrix.[21,22] These results indicated that the inhibition of cell proliferation, invasion, and migration in response to siRNA-RPN2 treatment may be mediated via the regulation of caspase-3, caspase-9, E-cadherin, and MMP2. PI3K/AKT signaling plays [illegible] roles in cell proliferation, migration, and invasion of human NPC.[23,24] Our study showed that the phosphorylation of PI3K and AKT was blocked by siRNA-RPN2.

Conclusion

Our study showed that RPN2 was highly expressed in human NPC tissues. Additionally, the mRNA and protein levels of RPN2 were upregulated in the NPC cell lines, namely CNE2 and HNE1. Furthermore, siRNA-RPN2 can markedly inhibit the invasion and migration of NPC cells by regulating caspase-3, caspase-9, E-cadherin, and MMP2 expression, and PI3K/AKT signaling. RPN2, therefore, may serve as a biomarker for the diagnosis and prognosis of NPC. Finally, targeting the PI3K/AKT signaling pathway may be an effective therapeutic strategy for treating NPC.

Disclosure

The authors report no conflicts of interest in this work.

References

1. Fountzilas G, Psyrri A, Giannoulatou E, et al. Prevalent somatic BRCA1 mutations shape clinically relevant genomic patterns of nasopharyngeal carcinoma in Southeast Europe. *Int J Cancer*. 2018;142(1):66–80.
2. Chee J, Loh KS, Tham I, et al. Prognostic stratification of patients with metastatic nasopharyngeal carcinoma using a clinical and biochemical scoring system. *J Cancer Res Clin Oncol*. 2017;143(12):2563–2570.
3. Hsu C, Lee SH, Ejadi S, et al. Safety and antitumor activity of pembrolizumab in patients with programmed death-ligand 1-positive nasopharyngeal carcinoma: results of the KEYNOTE-028 study. *J Clin Oncol*. 2017;35(36):4050–4056.
4. Wang M, Liu G, Shan GP, Wang BB. In vivo and in vitro effects of ATM/ATR signaling pathway on proliferation, apoptosis, and radiosensitivity of nasopharyngeal carcinoma cells. *Cancer Biother Radiopharm*. 2017;32:193–203.
5. Ou X, Miao Y, Wang X, Ding J, He X, Hu C. The feasibility analysis of omission of elective irradiation to level IB lymph nodes in low-risk nasopharyngeal carcinoma based on the 2013 updated consensus guideline for neck nodal levels. *Radiat Oncol*. 2017;12:137.
6. Meng H, Zhu X, Li L, et al. Identification of CALM as the potential serum biomarker for predicting the recurrence of nasopharyngeal carcinoma using a mass spectrometry-based comparative proteomic approach. *Int J Mol Med*. 2017;40:1[illegible]2–1164.
7. Chen WB, Zhang B, Liang L, et al. To predict the radiosensitivity of nasopharyngeal carcinoma using [illegible]ravoxel incoherent motion MRI at 3.0 T. *Oncotarget*. 2017;8:[illegible]740–5[illegible]50.
8. Fujita Y, Yagishita S, Tag[illegible]shita F, Yamamoto Y, [illegible]wano K, Ochiya T. Prognostic and therapeutic impact of RPN2-[illegible]ated tumor malignancy in non-small-cell lung cancer. *Oncotarget*. 2015;6:3335–3345.
9. Lu X, Nowicka U, Sridharan V, et al. Structure of the Rpn13-Rpn2 complex provides insights for Rpn13 and Uch37 as anticancer targets. *Nat Commun*. 2017;8:15540.
10. Zhang [illegible], Yan B, [illegible]ath SS, et al. Integrated transcriptional profiling and genomic analyses reveal RPN2 and HMGB1 as promising biomarkers in colorectal cancer. *Cell Biosci*. 2015;5:53.
11. Chen X, Yue B, Zhang C, et al. MiR-130a-3p inhibits the viability, proliferation, invasion, and cell cycle, and promotes apoptosis of nasopharyngeal carcinoma cells by suppressing BACH2 expression. *Biosci Rep*. 2017;37:pii.
12. [illegible]g G, Li C. miR-124 suppresses proliferation and invasion of nasopharyngeal carcinoma cells through the Wnt/beta-catenin signaling pathway by targeting Capn4. *Onco Targets Ther*. 2017;10:2711–2720.
13. Wang JY, Jin X, Li XF. Knockdown of TMPRSS3, a transmembrane serine protease, inhibits the proliferation, migration, and invasion in human nasopharyngeal carcinoma cells. *Oncol Res*. 2018;26(1):95–101.
14. Jiang C, Zhou L, Wang H, Zhang Q, Xu Y. Axl Is a Potential Cancer Prognostic Marker for the Migration and Invasion of Nasopharyngeal Carcinoma. *Adv Clin Exp Med*. 2016;25:531–537.
15. Hsu CC, Huang SF, Wang JS, et al. Interplay of N-Cadherin and matrix metalloproteinase 9 enhances human nasopharyngeal carcinoma cell invasion. *BMC Cancer*. 2016;16:800.
16. Oudejans JJ, Harijadi A, Cillessen SA, et al. Absence of caspase 3 activation in neoplastic cells of nasopharyngeal carcinoma biopsies predicts rapid fatal outcome. *Mod Pathol*. 2005;18:877–885.
17. Zhang Z, Bu X, Chen H, Wang Q, Sha W. BMI-1 promotes the invasion and migration of colon cancer stem cells through the downregulation of E-cadherin. *Int J Mol Med*. 2016;38:1199–1207.
18. Cheng JC, Chang HM, Xiong S, So WK, Leung PC. Sprouty2 inhibits amphiregulin-induced down-regulation of E-cadherin and cell invasion in human ovarian cancer cells. *Oncotarget*. 2016;7:81645–81660.
19. Li Y, Huang Y, Qi Z, Sun T, Zhou Y. MiR-338-5p promotes glioma cell invasion by regulating TSHZ3 and MMP2. *Cell Mol Neurobiol*. 2018;38:669–677.
20. Xu W, Xu H, Fang M, Wu X, Xu Y. MKL1 links epigenetic activation of MMP2 to ovarian cancer cell migration and invasion. *Biochem Biophys Res Commun*. 2017;487:500–508.
21. Yang H, Liang J, Zhou J, et al. Knockdown of RHOC by shRNA suppresses invasion and migration of cholangiocellular carcinoma cells via inhibition of MMP2, MMP3, MMP9 and epithelial-mesenchymal transition. *Mol Med Rep*. 2016;13:5255–5261.
22. Ghosh A, Dasgupta D, Ghosh A, et al. MiRNA199a-3p suppresses tumor growth, migration, invasion and angiogenesis in hepatocellular carcinoma by targeting VEGFA, VEGFR1, VEGFR2, HGF and MMP2. *Cell Death Dis*. 2017;8:e2706.

23. Xie M, Yi X, Wang R, et al. 14-Thienyl methylene matrine (YYJ18), the derivative from matrine, induces apoptosis of human nasopharyngeal carcinoma cells by targeting MAPK and PI3K/Akt pathways in vitro. *Cell Physiol Biochem*. 2014;33:1475–1483.

24. Wong CH, Ma BB, Cheong HT, Hui CW, Hui EP, Chan AT. Preclinical evaluation of PI3K inhibitor BYL719 as a single agent and its synergism in combination with cisplatin or MEK inhibitor in nasopharyngeal carcinoma (NPC). *Am J Cancer Res*. 2015;5:1496–1506.